Human Molecular Genetics, 2017, Vol. 26, No. 12 2207–2217

doi: 10.1093/hmg/ddx110
Advance Access Publication Date: 13 April 2017
Original Article

ORIGINAL ARTICLE

P4HA1 mutations cause a unique congenital disorder of connective tissue involving tendon, bone, muscle and the eye

Yaqun Zou[1,†], Sandra Donkervoort[1,†], Antti M. Salo[2,†], A. Reghan Foley[1], Aileen M. Barnes[3], Ying Hu[1], Elena Makareeva[4], Meganne E. Leach[1,5], Payam Mohassel[1], Jahannaz Dastgir[1], Matthew A. Deardorff[6], Ronald D. Cohn[7], Wendy O. DiNonno[8], Fransiska Malfait[9], Monkol Lek[10], Sergey Leikin[4], Joan C. Marini[3], Johanna Myllyharju[2] and Carsten G. Bönnemann[1,*]

[1]Neuromuscular and Neurogenetic Disorders of Childhood Section, National Institute of Neurological Disorders and Stroke, National Institutes of Health, Bethesda, MD, USA, [2]Oulu Center for Cell-Matrix Research, Biocenter Oulu, Faculty of Biochemistry and Molecular Medicine, Oulu, Finland, [3]Section on Heritable Disorders of Bone and Extracellular Matrix, Eunice Kennedy Shriver National Institute of Child Health and Human Development, National Institutes of Health, Bethesda, MD, USA, [4]Section on Physical Biochemistry, Eunice Kennedy Shriver National Institute of Child Health and Human Development, National Institutes of Health, Bethesda, MD, USA, [5]Children's National Health System, Washington, DC, USA, [6]Division of Human Genetics, Department of Pediatrics, The Children's Hospital of Philadelphia, Perelman School of Medicine at the University of Pennsylvania, Philadelphia, PA, USA, [7]Division of Clinical and Metabolic Genetics, Centre for Genetic Medicine, The Hospital for Sick Children, Toronto, ON, Canada, [8]Department of Maternal-Fetal Medicine, Eastern Virginia Medical School, VA, USA, [9]Center for Medical Genetics, Ghent University Hospital and Ghent University, De Pintelaan 185, B-9000 Ghent, Belgium and [10]Analytic and Translational Genetics Unit, Massachusetts General Hospital, Boston, MA, USA

* To whom correspondence should be addressed at: Neuromuscular and Neurogenetic Disorders of Childhood Section, Neurogenetics Branch, National Institute of Neurological Disorders and Stroke/NIH, Porter Neuroscience Research Center, 35 Convent Drive, Bldg 35, Room 2A-116, Bethesda, MD 20892-3705, USA. Tel: +1 3015945496; Fax: +1 3014803365; Email: carsten.bonnemann@nih.gov

Abstract

Collagen prolyl 4-hydroxylases (C-P4Hs) play a central role in the formation and stabilization of the triple helical domain of collagens. *P4HA1* encodes the catalytic α(I) subunit of the main C-P4H isoenzyme (C-P4H-I). We now report human bi-allelic *P4HA1* mutations in a family with a congenital-onset disorder of connective tissue, manifesting as early-onset joint hypermobility, joint contractures, muscle weakness and bone dysplasia as well as high myopia, with evidence of clinical improvement of motor function over time in the surviving patient. Similar to *P4ha1* null mice, which die prenatally, the muscle tissue from

[†]These authors contributed equally to this work.
Received: October 20, 2016. **Revised:** March 15, 2017. **Accepted:** March 16, 2017

P1 and P2 was found to have reduced collagen IV immunoreactivity at the muscle basement membrane. Patients were compound heterozygous for frameshift and splice site mutations leading to reduced, but not absent, P4HA1 protein level and C-P4H activity in dermal fibroblasts compared to age-matched control samples. Differential scanning calorimetry revealed reduced thermal stability of collagen in patient-derived dermal fibroblasts versus age-matched control samples. Mutations affecting the family of C-P4Hs, and in particular C-P4H-I, should be considered in patients presenting with congenital connective tissue/myopathy overlap disorders with joint hypermobility, contractures, mild skeletal dysplasia and high myopia.

Introduction

Collagenopathies are a phenotypically and genetically heterogeneous group of disorders caused by various defects in collagen formation. There is growing recognition that the underlying pathophysiological mechanisms in many of these disorders are connected by virtue of their effects on matrix collagens, caused by a deficiency of, or dominant negative effects on, (pro)collagens or by an expanding group of collagen biosynthesis and modifying proteins (1). Collagen prolyl 4-hydroxylases (C-P4Hs) (EC 1.14.11.2) play a central role in the synthesis of collagens. C-P4Hs catalyze the formation of 4-hydroxyproline through hydroxylation of the proline residues of the -Gly-X-Pro- repetitive motif in collagen and collagen-like proteins, which are essential for the formation and stabilization of the collagen triple helical domain (2–4). C-P4Hs reside in the lumen of the endoplasmic reticulum (ER) and form as $\alpha_2\beta_2$ tetramers, composed of chaperone protein disulfide isomerase (PDI) as the β subunit and one of three α isoforms (I, II, or III) serving as the catalytic α subunits (5–9). PDI is encoded by *P4HB*, and a heterozygous missense mutation in *P4HB* has been reported to cause Cole-Carpenter syndrome, a bone fragility disorder with craniosynostosis and ocular proptosis (10). C-P4H α(I) (encoded by *P4HA1*) is the main isoform in most cells, while C-P4H α(II) (encoded by *P4HA2*) is the predominant isoform in chondrocytes, osteoblasts and endothelial cells (11,12). *P4HA3*, encoding C-P4H α(III), is expressed in many tissues but at a lower level than *P4HA1* and *P4HA2* (8). In *P4HA1*, two forms of mRNA are generated by mutually exclusive alternative splicing of the two consecutive homologous 71-bp exons 9 and 10. Both species of mRNA are expressed in all tissues studied (highest in skeletal muscle, lowest in the brain), but preferential expression of exon 9 versus 10 in various tissues has been reported (5,13). C-P4Hs I to III are highly conserved across species. *P4ha1*$^{-/-}$ null mice are embryonically lethal with evidence of impaired assembly of collagen IV at the basement membrane, whereas *P4ha1*$^{+/-}$ mice have no abnormalities (14). In contrast, mice with inactivated α(II) subunit, *P4ha2*$^{-/-}$, have no apparent phenotypic abnormality, as C-P4H-I can to a large extent compensate for the lack of C-P4H-II. Interestingly, in *P4ha1*$^{+/-}$; *P4ha2*$^{-/-}$ mice, the combined partial inactivation of C-P4H-I and complete inactivation of C-P4H-II leads to a biomechanically impaired extracellular matrix. These mice are smaller than their littermates and display moderate chondrodysplasia and kyphosis (15).

As of yet no recessively inherited mutations in any of the enzymatically active C-P4H α -subunit genes had been identified as a cause of human disease. Here we report compound heterozygous mutations in *P4HA1* as a cause of a novel congenital-onset overlap syndrome of connective tissues involving bones, tendons, muscle and the eye, manifesting with joint hypermobility, contractures, congenital weakness, mild skeletal dysplasia without bone fragility and high myopia in a family with two affected siblings. As a result of the combined frameshift and splice site mutations, a significant reduction of total C-P4H activity and C-P4H α(I) protein were observed in patients-derived fibroblasts compared to age-matched controls. Collagen isolated from cultured dermal fibroblasts was of lower thermal stability, due to a reduction in proline hydroxylation of the collagen triple helical domain in *P4HA1* patients.

Results

Clinical findings

The proband (P1) is an 8-year-old male born to non-consanguineous parents of Chinese descent. First concerns arose prenatally at a routine ultrasound at 20 weeks of gestation, which showed contractures of the joints, with the knees and elbows in a fixed position in all fetal scans (images are not available). Prenatal movements were present on all subsequent ultrasound examinations. He was born at 40 weeks and 3 days by Cesarean section due to failure to progress. Apgars were 7 and 9. Birth weight was 3320 grams (50th percentile for ethnic Chinese newborns), and birth length was 48 centimeters (8.5th percentile for ethnic Chinese newborns). Both axial and appendicular hypotonia were noted with particularly pronounced low tone distally in the wrists without any movement except for thumb flexion and extension. There were no swallowing or breathing concerns. He had delayed motor development and started sitting when placed at age 9 months, standing at age 1.5 years, taking steps with support at age 2 years, walking in braces at age 3 years and walking independently at age 4 years.

On examination at age 7 ½ years, P1 had high myopia [−14.50 (OD) and −19.50 (OS)], macrocephaly (head circumference > 98% for age), low weight (weight < 3% for age) and small stature (height <3% for age). He had mild dysmorphic features with a broad nasal bridge, flat midface, mild frontal bossing, and retroverted ears, as demonstrated in clinical images taken at 6 ½ years of age (Fig. 1A and B) . He had camptodactyly, with notable webbing of fingers and absent flexor creases (Fig. 1C and D). He had flat arches and prominent calcanei. There was facial weakness with bilateral ptosis, endgrade limitation of upgaze, ocular proptosis, a high-arched palate and a transverse smile (Fig. 1E). Skin was soft and velvety. He had hypotonia which was prominent distally. He had joint contractures at the hips, knees, elbows, wrists, and the metacarpophalangeal and proximal interphalangeal joints of the hands, with hypermobility of the distal interphalangeal joints of the hands as well as hypermobility of the ankles and toes. Thumbs were maintained in a position of adduction (Fig. 1C and D). Despite his hand positioning, he was able to draw a very detailed picture with a regular pen, holding the pen between the thumb and palm of the hand. Deep tendon reflexes were absent, except at the biceps (1+). He stood with a lordotic and wide-based stance and had thoracic spinal rigidity with mild, asymmetric (left-greater-than-right-sided) scapular winging.

P1 demonstrated a notable improvement in strength over time. At the time of first clinical assessment at 3 ½ years of age, he was unable to maintain strength against gravity for neck and

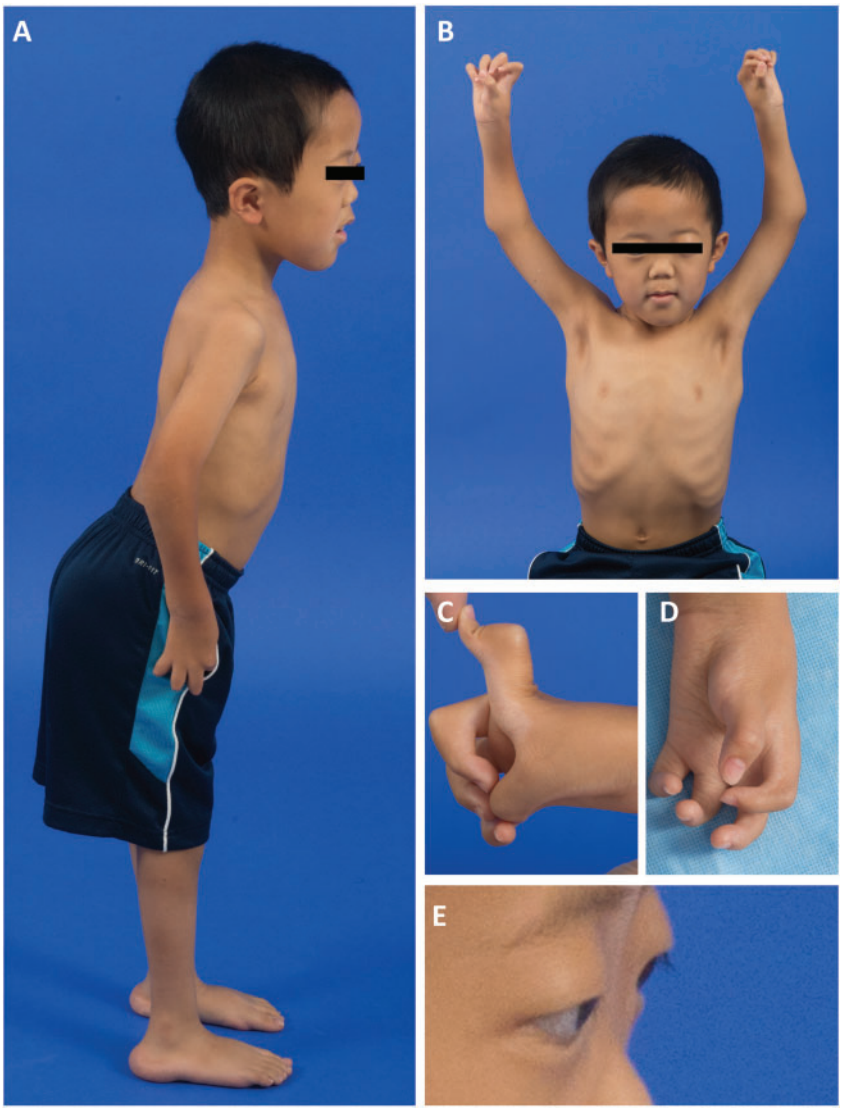

Figure 1. Clinical features of the proband (P1) at age 6½ years. (**A**) P1 with a lordotic stance, flat feet and elbow contractures. (**B**) Note macrocephaly (> 90th % for age), a broad nasal bridge, a flat midface, frontal bossing, and an asymmetric pectus carinatum (left > right). (**C** and **D**) Significant webbing between fingers limiting finger extension, joint hypermobility and absent flexor palmar creases of the hands. (**E**) Evidence of ocular proptosis and ptosis.

trunk flexion which subsequently improved to antigravity strength by 6 ½ years of age. Manual muscle testing revealed that muscle strength was full proximally and had improved distally, between 6 ½ years and 7 ½ years [Medical Research Council (MRC) grades] as follows: elbow extension 4/5 to 4+/5; wrist flexion 3/5 to 4/5; wrist extension 3/5 to 4/5; and hand grip 3+/5 to 4+/5 (within range of motion). Lower extremity distal strength remained weak with dorsiflexion 2/5, ankle inversion 3/5 and ankle eversion 3/5. At 7 ½ years, P1 was able to arise from the floor by rolling from supine to prone and arising without using his arms to a broad stance. He ambulated with a waddling-type gait with his left foot internally rotated and bilateral foot drop. He could accelerate his walking gait but could not achieve a run. Cognition was normal, and speech was hypophonic but fluent.

Serum creatine kinase (CK) level was performed at 1 year of age and was found to be mildly elevated (358 IU/L). Skeletal radiographic survey at age 3 years 9 months showed diffuse osteopenia, Wormian bones (intra-sutural bones) of the skull, and thinning with slight bowing and waviness of the bones with subtle metaphyseal changes (Fig. 2A–C), which seems to have improved on a repeat survey at age 6½ years (Fig. 2D). Muscle magnetic resonance imaging (MRI) performed of the lower extremities at 6 ½ years revealed relative preservation of the muscles above the knee except for some evidence of abnormally increased T1 signal within the vastus lateralis muscle bilaterally (Fig. 2E) compared to healthy control (Fig. 2G). In contrast, there was evidence of severely increased signal on T1-weighted sequences in all muscles below the knees bilaterally, suggestive of replacement of skeletal muscle with connective tissue and/or adipose tissue (Fig. 2F) compared to healthy control (Fig. 2H). Electromyography performed of the biceps brachii, vastus lateralis and tibialis anterior muscles was reported as normal and noted the very small size of the tibialis anterior muscle.

When the proband (P1) was 4 years of age, a subsequent male pregnancy (P2) was found to have bilateral clubfeet on fetal ultrasound at 19 weeks of gestation. A follow-up ultrasound

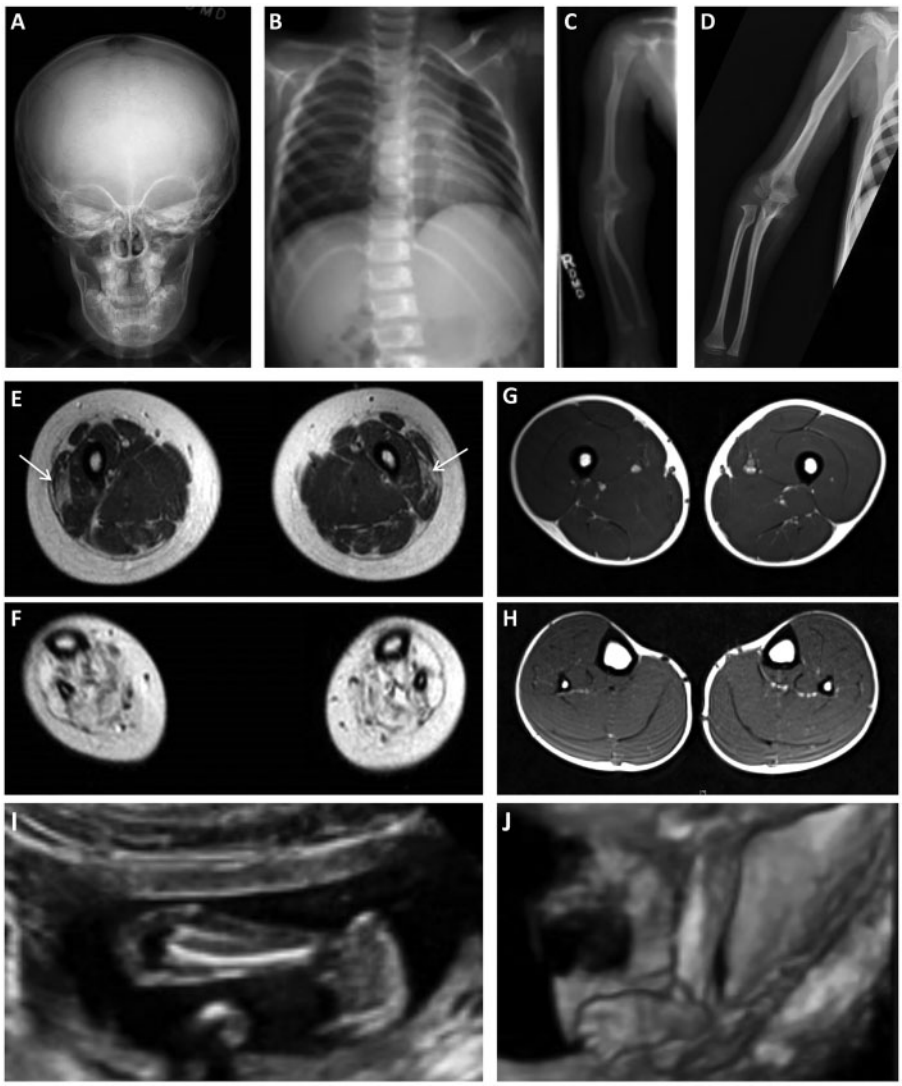

Figure 2. (**A–C**) Skeletal survey performed at the age 3 years in P1 revealing osteopenia. (A) Anterior-posterior (AP) view of skull with evidence of Wormian bones and a flattened AP diameter of the facial bones. (B) Ribs (AP, oblique) appear thin and slightly angulated. (C) On AP view of the long bones of the forearm, there is evidence of angulation of the right radius and ulna, and the distance between the proximal radius and distal humerus appears possibly increased. (**D**) Skeletal survey repeated at age 6½ years demonstrating improved osteopenia on AP view of the long bones of the forearm. (E-H) Muscle MRI. Lower extremity muscle MRI performed at age 6½ years in P1 (**E** and **F**) revealing abnormal signaling in the vastus lateralis bilaterally (E; arrows) and some atrophy of the quadriceps group but otherwise more normal-appearing muscle above the knee. In contrast, all of the muscles below the knee show severely abnormal signaling, suggestive of replacement of the muscle with connective tissue and/or adipose tissue (F). Muscle MRI in a patient without muscle disease demonstrating normal size and signaling of the muscles above the knee (**G**) and the muscles below the knee (**H**). (I and J) Fetal ultrasound images of P2. (I) At 19 weeks gestational age there was evidence of talipes equinovarus. (J) A follow-up fetal ultrasound performed at 21 weeks gestational age revealed continued abnormal posturing of the feet.

performed at 21 weeks of gestation revealed abnormal posturing and a flaccid appearance of the hands and feet as well as a lack of fetal tone (Fig. 2I and J). Amniotic fluid volume appeared normal, and estimated fetal weight was 405 grams (20% percentile). The genetic etiology as well as the clinical prognosis of P1's condition had remained undetermined at the time of this subsequent pregnancy, which the parents elected to terminate.

Family history was significant for two prior miscarriages and high myopia in the mother [−8 (OD) and −10 (OS)] and low myopia in the father [−2 (OD) and −2.5 (OS)]. There is one unaffected sibling age 12 months, who does not appear to be nearsighted; however, she has not had formal opthalmological testing. The maternal aunt and grandfather are reported to have moderate myopia, each between −4 and −6 diopters. There is a paternal uncle with low myopia [−2 (OD) and (−2.5 (OS)]; however, both paternal grandparents are not nearsighted.

Mutation analysis

Whole exome sequencing (WES) of P1 and P2 followed by variant filtering for call quality, rarity and predicted pathogenicity yielded two heterozygous mutations in *P4HA1*: a heterozygous splice donor site mutation (c.1543 + 2 T > G; NM_001017962.2) predicted to cause skipping of exon 12, and a heterozygous two-base pair insertion in exon 9 (c.1323_1324insAG; NM_001017962.2) predicted to result in a frameshift and premature stop codon (Fig. 3). Neither mutation had been previously reported, and neither was present in dbSNP, NHLBI EVS or ExAC Browser (16,17). Targeted

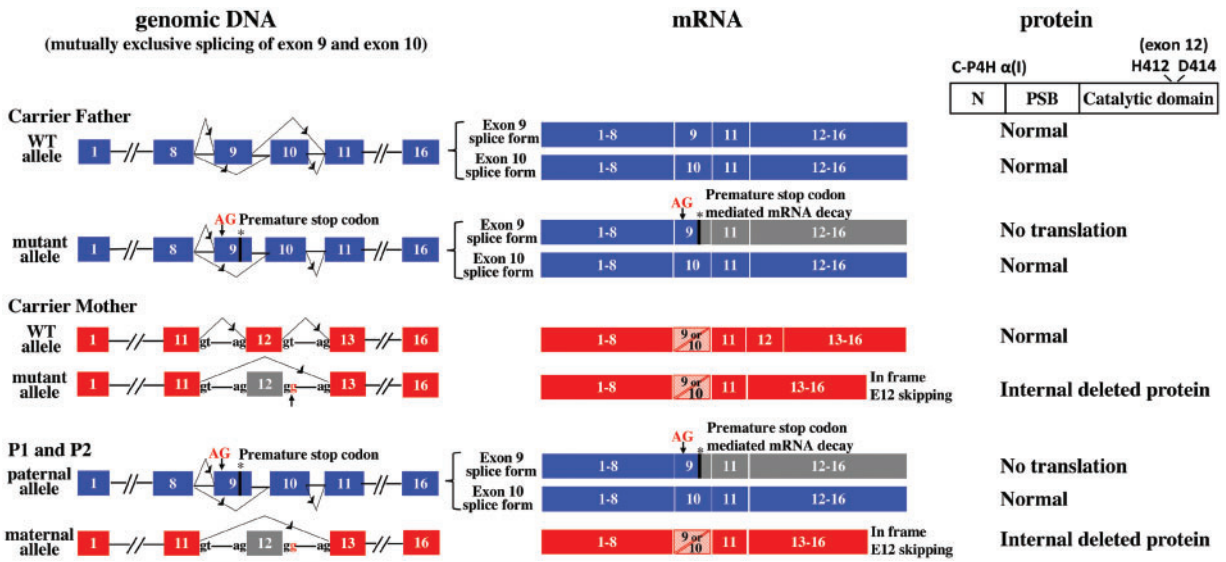

Figure 3. Schematic of *P4HA1* mutations and consequence at mRNA and protein level. Paternal wild type and mutant allele are shown on top (blue): Each allele has mutually exclusive exon 9 and exon 10 splice forms. The two-base pair insertion in exon 9 [c.1323_1324insAG; p.Arg362Glyfs*9; NM_001017962.2] leads to a premature stop of the exon 9 splice form, as a result this transcript is eliminated by NMD and no protein is translated. Due to the mutually exclusive alternative splicing of exon 9 and 10, the exon 10 containing splice form remains wild type sequence. Maternal wild type and mutant allele are shown in the middle (red): the splice donor site mutation [c.1543 + 2 T > G; p.Ala418_Arg434del; NM_001017962.2)] causes exon 12 skipping and an internally deleted protein. P1 and P2 inherited the paternal and maternal mutant alleles (bottom), as a result, the only normal C-P4H α (I) is translated from the exon 10 splice form of the mutant paternal allele.

parental segregation testing confirmed that the splice donor site mutation was inherited from the carrier mother, and the insertion mutation was inherited from the carrier father.

The effect of these mutations at the transcript level was further analysed using cDNA synthesized from RNA of dermal fibroblast of patients (P1, P2) and carrier parents. A pair of primers spanning the exon 12 transcript was used to confirm the effect of the maternal mutation on splicing (Supplementary Material, Table S1). Gel electrophoresis of the PCR fragment revealed an additional smaller band of equal intensity as the normal band in samples of P1, P2 and their mother, compared to the father and disease control (data not shown). Sequencing confirmed that the smaller band was derived from a mutant transcript in which exon 12 was skipped.

As *P4HA1* exon 9 and exon 10 undergo mutually exclusive alternative splicing (5,13), cDNA synthesized from RNA of dermal fibroblasts were used to analyse the effect of the paternal two base pair insertion with specific primers for the exon 9 splice form (Supplementary Material, Table S1 and Fig. S3). In the exon 9 retaining transcript the two nucleic acid insertion in exon 9 is expected to result in a frameshift generating a premature stop codon within exon 9, so that the transcript is predicted to potentially be degraded by nonsense-mediated decay (NMD). Using cDNA prepared from untreated fibroblasts of P1, P2 and carrier father, the mutation was not detectable, consistent with the presence of NMD. Mutation analysis with the cDNA prepared from cycloheximide (CHX) treated fibroblasts to suppress NMD, then confirmed the presence of the c.1323_1324insAG mutation in both P1, P2 and carrier father.

Muscle biopsy analysis

Muscle histology from P1's biopsy at age 2 years from the left quadriceps showed myofiber atrophy, with mild type 1 hypotrophy, an increase in interstitial endomysial connective tissue and mild fibrosis (Supplementary Material, Fig. S1). Immunohistochemical analysis of muscle tissue from P1 and P2 showed reduced immunoreactive staining for collagen IV as well as laminin γ1 in the muscle basement membrane (Fig. 5A).

C-P4H activity assay and western blot

The amount of total C-P4H activity in patient-derived fibroblasts was found to be reduced to approximately 50% of age-matched controls. There was only a slight reduction (approximately 10%) of activity in the mother's fibroblasts and a normal activity in the father's fibroblasts (Fig. 4A). C-P4H α(I) Western blot revealed a significant reduction of C-P4H α(I) protein in both affected siblings but no significant change in either parent compared to controls (Fig. 4B). In contrast, there was no significant difference in protein amount for C-P4H α(II) by Western blot analysis among all tested samples, indicating C-P4H α(II) expression was not up-regulated to compensate for the reduction of C-P4H α(I) expression (Fig. 4B).

When C-P4H α (I) Western blot analysis was performed with longer gel electrophoresis, two bands were revealed in the two affected siblings and the carrier mother (Supplementary Material, Fig. S2A). One band is of normal molecular weight and the other is smaller. As the c.1323_1324insAG mutation in paternal allele is located in alternatively spliced exon 9, the exon 10 containing transcript is expected to be intact. The normal sized band in two affected siblings is predicted to represent the protein product of the paternal exon 10 splice form, but with reduced expression level compared with age-matched disease controls which have both exon 9 and exon 10 splice forms. Based on the mutation analysis, the smaller band is predicted to correspond to the internally deleted protein translated from the maternal allele with exon 12 skipping. In both affected siblings, the smaller band had similar reduced intensity as the normal sized exon 10 splice form from the paternal allele; however, in the heterozygous mother, the smaller mutant band is much weaker than the normal band. The relatively lower expression

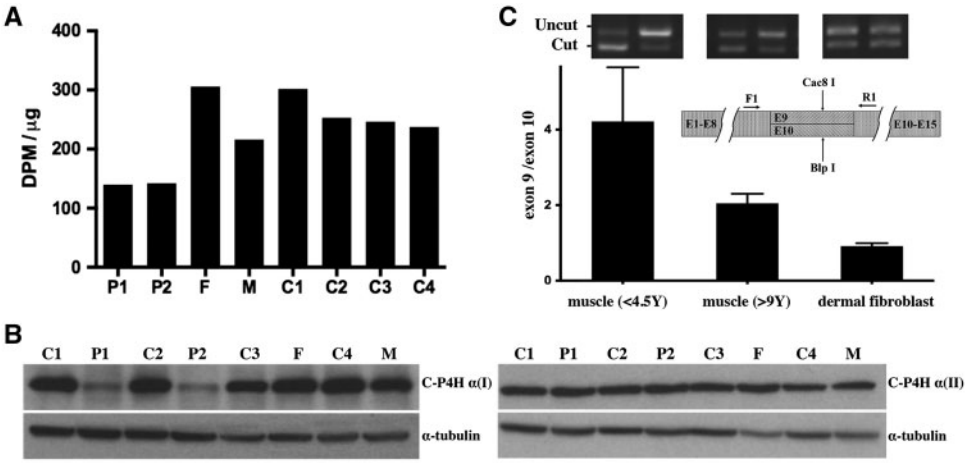

Figure 4. (**A**) Total C-P4H activity was reduced in cultured fibroblasts from *P1* and *P2* compared to age-matched controls (*C1* and *C2*). Activities in both carrier father (*F*) and carrier mother (*M*) were within normal range, although it was at the lower end of the range in the carrier mother. (**B**) Western blot analysis with α-tubulin loading control. C-P4H α (I) protein is reduced in patients-derived fibroblasts compared to age-matched controls (*C1* and *C2*). There is no up-regulation of C-P4H α (II) protein in cultured fibroblasts from *P1*, *P2* and their parents compared to controls. (**C**) Ratio of exon 9 versus exon 10 splice form in muscle tissue and cultured dermal fibroblasts from individuals of different ages as determined by RT-PCR followed with Cac8I (specific for exon 9) or BlpI (specific for exon 10) digestion. The exon 9 splice form is the major form expressed in muscle tissue, the average ratio of exon 9/exon 10 is 4.22 (SEM = 0.59) in younger individuals (<4.5 years), the average ratio of exon 9/exon 10 is 2.05 (SEM = 0.09) in older individuals (9 years to adult). The expression levels of exon 9 and exon 10 splice form are relatively equal in dermal fibroblasts at all ages tested (ranges from 8 months to adult, average ratio of exon 9/exon 10 = 0.92, SEM = 0.03).

level of the smaller mutant band in both affected siblings and their carrier mother indicates that the internally deleted C-P4H α(I) may be prone to degradation. We also confirmed by EndoH digestion that the molecular weight difference between the two bands is not due to abnormal N-glycosylation in the ER. (Supplementary Material, Fig. S2B)

Posttranslational modification and thermal stability of type I collagen

Type I collagen, the major collagen in skin and bone, would be predicted to also be affected by the reduction in C-P4H α(I) function. Migration of type I collagen synthesized from P1 and P2 fibroblasts, examined by SDS-urea PAGE, showed that the alpha 1 chain of type I collagen from both P1 and P2 fibroblasts migrated slightly faster than the control (Fig. 5B). As variations in collagen migration are frequently caused by changes in hydroxylation and glycosylation, hydroxylysine and hydroxyproline levels in the cultures were measured by amino acid analysis. Collagen proline 4-hydroxylation levels were decreased from 43.8% in control to 34% in P1, consistent with a decrease in C-P4H α(I). Interestingly, however, lysine hydroxylation was increased from 20.8% in control to 32.6% in P1 (Fig. 5C). This increase in lysine hydroxylation is not caused by slower collagen folding, since an intracellular assay of collagen folding did not reveal a difference, nor was collagen secretion found to be reduced in the context of the altered modification (Supplementary Material, Fig. S4).

Proline 4-hydroxylation is known to contribute significantly to collagen thermal stability, as collagens lacking 4-Hyp are not stable at 37°C (18). Differential scanning calorimetry (DSC) revealed ~1.3°C decrease in the thermal stability of type I collagen in the patient samples. A broadened and skewed collagen denaturation peak indicated the presence of a heterogeneous mix with respect to extent and/or sites of the posttranslational modification (Fig. 5D).

Differential expression of the alternatively spliced exon 9 and 10 of *P4HA1* in muscle tissue and dermal fibroblasts from individuals of different ages

Tissue and age-dependent differential expression of the two *P4HA1* alternatively spliced forms containing either exon 9 or 10 was analysed with a semi-quantitative assay based on unsaturated PCR followed by Cac8I (specific for exon 9) or BlpI (specific for exon 10) digestion. This analysis revealed that in cultured dermal fibroblasts derived from individuals of different ages, the exon 9 and 10 splice forms were expressed at similar level at all tested ages (ranges from 8 months to adult, average ratio of exon 9/exon 10 = 0.92, SEM = 0.03) (Fig. 4C). In contrast, the expression level of the exon 9 splice form was higher compared to the exon 10 splice form in muscle biopsy tissue across all tested ages (ranges from 4 months to adult). However, the difference was more pronounced in muscle samples from individuals of younger age (<4.5 year, average ratio of exon 9/exon 10 = 4.22, SEM = 0.59) than those in individuals older than age 9 years (average ratio of exon 9/exon 10 = 2.05, SEM = 0.09) (Fig. 4C). This result suggests that the exon 9 splice form is the major form expressed in muscle tissue, in particular in younger ages (below approximately age 4.5 years), while the difference between the two alternatively splice forms becomes less significant with increasing age, even though the exon 9 splice form remains the major form.

Discussion

Here we report compound heterozygous *P4HA1* activity reducing mutations in a family with two siblings affected with a novel collagenopathy, presenting as an overlap syndrome involving tendon, bone, muscle and the eye. Collagenopathies as prototypical disorders of the extracellular matrix encompass various subtypes, depending on clinical presentation, severity, tissue distribution and affected collagen subtype (19). The most notable example is osteogenesis imperfecta (OI) manifesting with bone and tissue fragility, caused by mutations in the primary

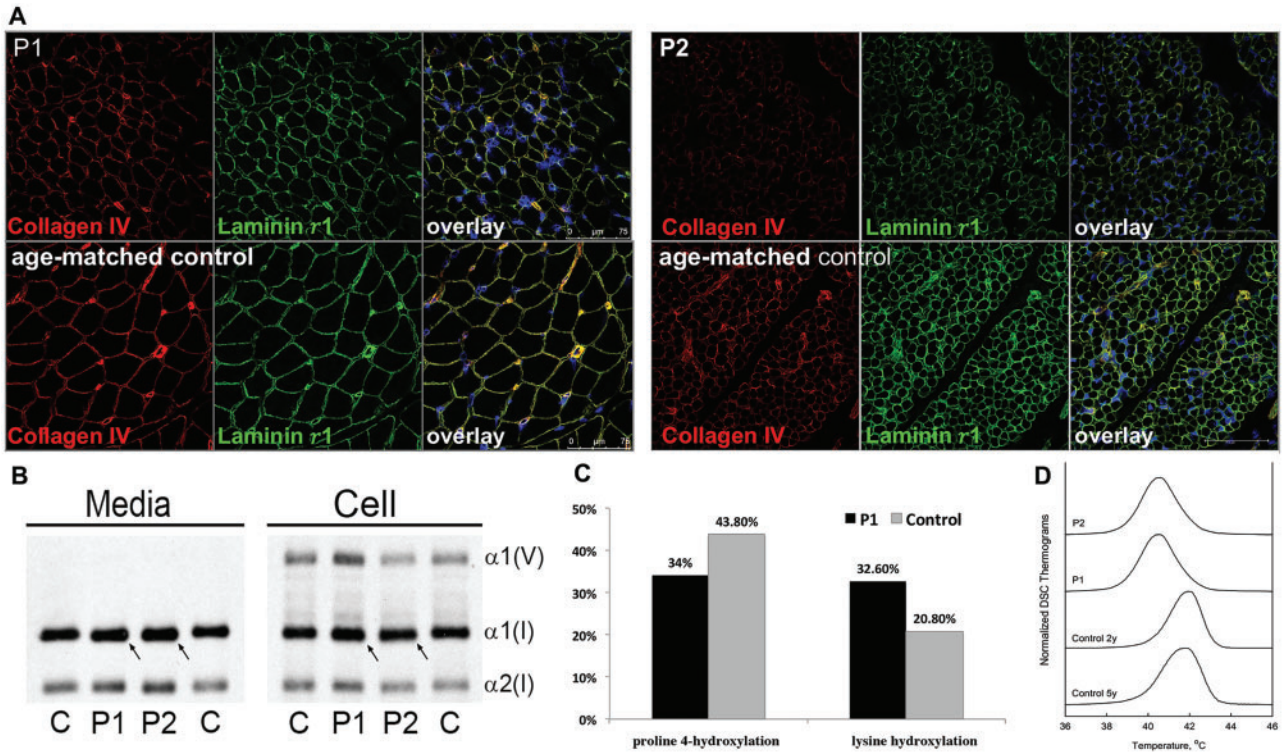

Figure 5. (**A**) In muscle biopsies of affected siblings *P1* and *P2*, the basement membrane stains continuously on immunohistochemistry, but both collagen IV and laminin $\gamma 1$ staining were reduced compared to age-matched controls. (**B**) Analysis of type I collagen protein shows slightly increased migration of media and cell layer collagens in *P1* and *P2* compared to control (*C*). (**C**) Collagen proline 4-hydroxylation levels were decreased from 43.8% in control (*C*) to 34% in proband (*P1*), consistent with the hypomorphic nature of the mutations; while lysine hydroxylation was increased from 20.8% in control to 32.6% in *P1*. (**D**) Differential scanning calorimetry (DSC) revealed apparent melting temperature T_m (temperature at the denaturation peak maximum) that was reduced ~1.3 °C in *P1* and *P2* (T_m = 40.5 °C in both) compared to 2 y.o, (T_m = 41.9 °C) and 5y.o. normal controls (T_m = 41.7 °C). The broadening and trailing edge of the *P1* and *P2* denaturation thermograms suggested the presence of a heterogenous population of type I collagen molecules with different thermal stabilities.

collagen in bone, type I, as well as in proteins that affect type I collagen folding, modification and processing (19,20). Additionally, Ehlers-Danlos syndromes (EDS) are a group of disorders of connective tissue characterized by joint hypermobility and skin hyperextensibility, and variable degrees of tissue fragility, frequently caused by mutations in collagens and collagen modifying genes (21). Patients with EDS can also present with congenital muscle hypotonia, muscle atrophy and delayed motor development similar to a primary myopathy (22,23). Finally, disorders caused by collagen type VI (*COL6*) dysfunction are in fact progressive muscular dystrophies that also manifest with distal joint hypermobility, proximal joint contractures and abnormal scar formation, clinical findings frequently seen as part of the spectrum of EDS, indicative of phenotypic overlap between various groups of collagen-related extracellular matrix disorders (24). Mutations in collagen modifying genes may additionally present with overlapping clinical features originating from various connective tissues and collagen species, as exemplified in the family reported here with compound heterozygous mutations in *P4HA1*.

The proband (P1) has a clinical presentation which partially overlaps with EDS type VIA (caused by mutations in *PLOD1*, encoding lysyl hydroxylase 1) and EDS musculocontractural type (formerly EDS type VIB) (caused by mutations in *CHST14*, encoding carbohydrate sulfotransferase 14), as these patients can also present with congenital hypotonia, muscle weakness, delayed motor milestones and joint hypermobility. Typically, muscle function improves with age in patients with these types of EDS, in contrast to what would be expected for a *COL6*-related muscle disease (Ullrich/Bethlem spectrum), in which there is a progressive decline in muscle and respiratory function (24). Unlike patients with EDS type VIA, P1 did not have any evidence of kyphoscoliosis or vascular rupture, and unlike patients with EDS musculocontractural type, P1 did not have tissue fragility, wrinkling of hands on the palms or joint dislocations. On a pathomechanistic level, both *PLOD1* and *CHST14* are similar to *P4HA1* in that they encode for collagen modifying proteins, with *PLOD1* responsible for hydroxylation of the lysine residues in the -Gly–X-Lys- sequences (a modification which also has a role in collagen glycosylation and crosslink formation) and *CHST14* responsible for the formation of the collagen fibrils through dermatan sulfate mediated electrostatic binding (25,26). Mutations in *PLOD2* (lysyl hydroxylase 2, causing Bruck syndrome 2 (27)) and *PLOD3* (lysyl hydroxylase 3, reported in one family (28)) have also been described, again with partial phenotypic overlap to our family, including clubfeet, osteopenia, Wormian bones in *PLOD2*, and flat face, shallow orbit, some myopia and muscle atrophy in *PLOD3*.

Here, we report compound heterozygous frameshift and splice site mutations in *P4HA1* that impair but not abolish C-P4H α(I) activity. The maternal *P4HA1* exon 12 splice donor site mutation causes an internally deleted C-P4H α(I). This mutant protein is detectable in the fibroblast cell lysate of both patients and the carrier mother by Western blot (Supplementary Material, Fig. S2A), but at a reduced level, possibly due to partial protein degradation. The two critical catalytic sites of H412 and

D414 are encoded in exon 12 (29,30). Therefore, based on studies of H412 and D414 mutant recombinant human C-P4H-I (31), the maternal mutant α(I) subunit is predicted to completely lack catalytic activity, even though it should still be capable of forming tetramers with the PDI/β subunit. On the paternal mutant allele, the two nucleic acid insertion in exon 9 results in a premature stop in the exon 9 *P4HA1* splice form, which is eliminated by nonsense-mediated mRNA decay. In both P1 and P2, carrying these compound heterozygous mutations in *P4HA1*, functional C-P4H α(I), is thus solely expressed from the exon 10 splice form of the mutant paternal allele. Therefore, the result is a reduction, but not a complete absence of normal C-P4H α(I) activity, resulting in a hypomorphic, rather than a loss-of-function situation.

Total C-P4H activity in the patients-derived dermal fibroblasts is less than 50% of that of age-matched controls along with a substantial reduction in C-P4H α(I) protein level (Fig. 4A and B). In addition, the Western blot data indicates that there is no compensatory up-regulation of C-P4H α(II) amount (Fig. 4B). The remaining C-P4H activity is thus likely to be contributed to by C-P4H-II and to a lesser extent by C-P4H-III, in addition to the low amount of normal C-P4H-I produced by the exon 10 splice form of the mutant paternal allele. The reduction of total C-P4H activity was found to lead to slightly increased mobility of alpha 1 chain of type I collagen (Fig. 5B), reduced proline 4-hydroxylation, increased lysine hydroxylation (Fig. 5C), and reduced thermal stability of secreted collagen in P1 and P2 fibroblasts (Fig. 5D). However, no significant abnormality was found in type I collagen folding and secretion in both patients' fibroblasts (Supplementary Material, Fig. S4). We speculate that under normal conditions C-P4H-I binding inhibits lysine hydroxylase (LH) binding at adjacent sites, slowing down, or even preventing some lysine hydroxylation. Reduced C-P4H-I would then indicate that there is less bound C-P4H-I, more LH binding and thereby result in more hydroxylysine (Hyl). The normal folding rate observed would prevent excessive Hyl glycosylation which is consistent with the nearly normal collagen mobility. Similar to our observations, in *P4ha1*$^{+/-}$; *P4ha2*$^{-/-}$ mice the underhydroxylated collagen still showed a normal mobility, indicating lack of hyperglycosylation, while impaired thermal stability of collagen fibrils as seen in our patients, was also observed in *P4ha1*$^{-/-}$ mice and *P4ha1*$^{+/-}$; *P4ha2*$^{-/-}$ mice (14,15).

The nature of muscle involvement in proband P1 is of interest as he presented with severe and generalized hypotonia and weakness, with manifestations in-utero as early as 20 weeks of gestation and evident at birth, but then demonstrated clinical improvement over time postnatally in the proximal muscles, while distal muscles remained severely involved clinically and by imaging. As the only functionally active C-P4H α(I) subunit is expressed by paternal exon 10 splice form, we hypothesized that changes in the ratio of use of the *P4HA1* alternative splice exons 9 and 10 in different tissues and during development may help explain the proband's clinical course of notable improvement in muscle strength over time. In contrast to the equal expression of exon 9 splice form and exon 10 splice form in cultured skin fibroblast from individuals of different ages, the exon 10 splice form is the comparatively minor splice form in muscle tissue, especially in early development stages, when most of P4H α(I) expression appears to be dependent on the exon 9 form, which in our patients includes the mutation. However, with increasing age the relative expression level of the exon 10 splice form also increases, in our case possibly resulting in a relative "rescue" at least in proximal muscles. The increasing residual expression from the paternal allele in our patients may be essential for viability of what would otherwise be a prenatally lethal condition, as the *P4ha1* null mice are embryonically lethal (14). Therefore, since it can be assumed that complete inactivation of *P4HA1* is not compatible with life, future mutations to be found in this gene in human would also be expected to be hypomorphic, rather than complete loss-of-function mutations. Due to this fine balance, C-P4H-I related diseases may be very rare. The relatively higher expression of the exon 10 splice form in cultured fibroblast compared to muscle also helps explain the milder clinical involvement of skin and the nonsignificant finding in procollagen proline hydroxylation, collagen folding and secretion in cultured dermal fibroblast. With the relatively lower exon 10 splice form expression in muscle tissue, it is notable that we observed reduced collagen IV immunoreactivity at the muscle basement membrane in patients' muscle biopsy.

The high myopia in the proband [-14.50 (OD) and -19.50 (OS)], his mother [-8 (OD) and -10 (OS)] and moderate myopia in the maternal aunt and grandfather is of interest, as C-P4Hs play a central role in collagen synthesis. High myopia in humans has been found to be associated with a thinner sclera characterized by a narrowing and dissociation of the collagen fiber bundles and a reduction in collagen fiber diameter (32,33). Among collagen disorders, this is a feature in Stickler syndrome, caused by mutations in *COL2A1*, *COL11A1* and *COL11A2*, and interestingly is also associated with a flat midface as seen in our patient (34–36). Dominant negative missense mutations in *P4HB* were reported to cause Cole-Carpenter syndrome, which is characterized by ocular proptosis in addition to frequent fractures, craniosynostosis, hydrocephalus and distinctive facial features (10). Mono-allelic missense and truncating mutations in *P4HA2* have been reported to cause non-syndromic high myopia (37). This association with high myopia indicates that C-P4Hs play a critical role in eye structure maintenance and development in human and that this structure may be particularly sensitive to activity changes in the enzymes. Therefore, the role of C-P4Hs in the development and function of the eye remains to be investigated.

Here we report human *P4HA1* mutations causing a congenital disorder of various connective tissues. The C-P4Hs are conserved enzymes essential for biosynthesis of collagens and collagen-like proteins that make up the major component of ECM. The unique mutations identified in our patients shed light on the normal function and alternative splicing of *P4HA1* in different tissues during development. Mutations affecting C-P4Hs should be considered in patients presenting with connective tissue/myopathy overlap disorders with features of Ehlers-Danlos syndromes.

Materials and Methods

Patient recruitment and sample collection

The study was approved by the Institutional Review Board of the National Institute of Neurological Disorders and Stroke, National Institutes of Health (Protocol 12-N-0095). Written informed consents were obtained by a qualified investigator. Medical history was obtained, and clinical evaluations were performed as part of the standard neurologic evaluation. DNA and tissue were obtained based on standard procedures.

Exome sequencing and mutation analysis

Whole exome sequencing on DNA obtained from blood (P1) and cultured skin fibroblast (P2) was performed at the NIH Intramural Sequencing Center using the Illumina (San Diego, CA) TruSeq Exome Enrichment Kit and Illumina HiSeq 2000 sequencing instruments. Variants were analysed using Varsifter and *Seqr* and searched for in dbSNP, NHLBI EVS, Exome Aggregation Consortium (ExAC Browser) (17,38).

Targeted *P4HA1* mutation analysis was further performed with cDNA prepared from dermal fibroblast, which were treated with 0.2 mg/ml cycloheximide (CHX) (Sigma, Saint Louis, Missouri) for 19 h to suppress nonsense-mediated mRNA decay. Primers were designed to amplify the specific transcript spanning the alternatively splice exon 9 or exon 10 and the transcript spanning exon 12 (Supplementary Material, Table S1).

Muscle biopsy analysis

Cold methanol fixed 9 μm muscle cross-sections were incubated with primary antibodies at 4 °C overnight (Collagen IV (MAB1430, Millipore, Billerica, MA), Laminin γ1 (L9393, Sigma, Saint Louis, Missouri), the antibody labeling was detected with secondary antibodies for 1 h at room temperature [Alexa 568-conjugated goat anti-mouse IgG and Alexa 488-conjugated goat anti-rabbit IgG (Thermofisher, Rockford, IL)]. Prepared muscle sections were imaged with a Leica SP5 confocal microscope (Leica, Wetzlar, Germany).

C-P4H activity assay and western blot

Cultured fibroblasts isolated from the two affected siblings, the parents and age-matched controls were washed twice with PBS and lysed with 0.1M NaCl, 0.1M glycine, 0.1% Triton X-100, 10 mM Tris pH 7.8 supplemented with EDTA-free complete protease inhibitors (Roche, Indianapolis, IN). Soluble fraction was obtained by centrifugation and the protein concentration was measured using the Bradford assay (Bio-Rad, Hercules, CA). Total C-P4H activity was determined by an assay that measures formation of 4-hydroxy [^{14}C] proline in a [^{14}C]proline-labeled protocollagen substrate consisting of nonhydroxylated pro-α chains of chick type I procollagen (39).

EndoH (New England Biolabs, Ipswich, MA) digestion was performed according to manufacturer's instructions. Aliquots of the lysates were analysed by Western Blot using 10% SDS-PAGE under reducing conditions followed by a transfer to PVDF membrane (Millipore, Billerica, MA) and incubation with antibodies against P4HA1 (12658-1-AP, Proteintech Group, Rosemont, IL) and P4HA2 (15). In order to resolve P4HA1 protein products from maternal and paternal allele, a 16cm long gel was used instead of a 5.5cm long one used in other assays.

Posttranslational modification and thermal stability of type I collagen

Cultured fibroblasts from the two affected siblings and a age-matched control were grown to confluence in 6-well culture dishes. Cells were incubated in serum-free media for 2 h, then labeled with 437.5 μCi/ml L-[2,3,4,5-^{3}H] proline in serum-free media for 18 h. Media and cell layer collagens were collected, precipitated by ammonium sulfate, and analysed by 6% SDS-urea-PAGE. The media and cell layer samples were balanced for equal signal to examine difference in type I collagen migration. Amino acid analysis was performed on secreted type I collagen by high pressure liquid chromatography (AIBiotech, Richmond, VA) to quantitate levels of 4-hydroxyproline, proline, hydroxylysine and lysine.

Collagen secreted by cultured fibroblasts was purified by pepsin treatment (0.1 mg/ml in 0.5 M acetic acid) followed by two rounds of selective precipitation with 0.7 M NaCl. Thermal stability (denaturation thermograms) of collagen suspended in 0.2 M sodium phosphate, 0.5 M glycerol, pH 7.4 (to prevent aggregation) was measured by differential scanning calorimetry in a Nano III DSC instrument (Calorimetry Sciences Corporation, Lindon, Utah) at 0.125 °C/min heating rate from 10 to 50 °C (40).

Inclusion of the alternatively spliced exon 9 and exon 10 of *P4HA1* in muscle tissue and in dermal fibroblasts from individuals of different ages

To study the expression of exon 9 and exon 10 *P4HA1* splice forms, we designed a semi-quantificative assay based on unsaturated PCR and splice form specific restrictive enzyme (RE) digestion (Supplementary Material, Table S1 and Fig. S3). cDNA was prepared from total RNA isolated from muscle tissue or from dermal fibroblast cultures of individuals of different ages. Both exon 9 and exon 10 alternatively spliced transcripts were unsaturated-PCR amplified simultaneously with a pair of common primers that span both exon 9 and exon 10. Equal amounts of PCR product were digested with either Cac8I or BlpI (New England Biolabs, Ipswich, MA). Cac8I has a cutting site in exon 9, but not in exon 10, while BlpI can cut exon 10 sequence only. Therefore, the uncut band from Cac8I digestion is a transcript from the exon 10 containing splice form (exon 10 splice form for short), the uncut band from BlpI digestion is a transcript from the exon 9 containing splice form (exon 9 splice form for short). Exon 9 and exon 10 splice form specific PCR products were used as RE digestion control to monitor the digestion efficiency. After the RE digestion was complete according to digestion controls, cut and uncut bands were separated in 2% agarose gel. Images of the separated bands were taken with Geldoc (Biorad, Hercules, CA), and intensity of the following bands was measured using image studio software (Li-Cor Inc, Lincoln, NE): exon 9 splice form (BlpI uncut band) and exon 10 splice form (Cac8I uncut band). The relative ratio of two splice forms is calculated as: exon 9 splice form/exon 10 splice form.

Supplementary Material

Supplementary Material is available at *HMG* online.

Web resources

The URLs for data presented herein are as follows: dbSNP, https://www.ncbi.nlm.nih.gov/projects/SNP/
NHLBI Exome Sequencing Project (ESP) Exome Variant Server, http://evs.gs.washington.edu/EVS/
Online Mendelian Inheritance in Man (OMIM), www.omim.org
Exome Aggregation Consortium, http://exac.broadinstitute.org
SEQR, https://seqr.broadinstitute.org

Acknowledgements

We thank the family for participating. Minna Siurua is acknowledged for expert technical assistance. We thank Dr Peter Byers for helpful discussion of the phenotype. We also thank the NIH Intramural Sequencing Center for performing the exome

sequencing; the Analytic and Translational Genetics Unit at Massachusetts General Hospital for their help in the exome analysis; the Exome Aggregation Consortium; and the groups that provided exome variant data for comparison. A full list of contributing groups can be found at http://exac.broadinstitute.org/about.

Conflict of Interest statement. None declared.

Funding

National Institute for Neurological Disorders and Stroke/National Institutes of Health. National Institutes of Health Intramural Research Program Funding from the National Institute of Neurological Disorders and Stroke (CGB) and National Institute of Child Health and Human Development (SL and JCM). FM is a senior Clinical Investigator at the Fund for Scientific Research, Flanders, Belgium. This study was supported by the Academy of Finland Center of Excellence 2012-2017 Grant 251314 (JM), the S. Jusélius Foundation (JM), and the Jane and Aatos Erkko Foundation (JM).

References

1. Mao, J.R. and Bristow, J. (2001) The Ehlers-Danlos syndrome: on beyond collagens. *J. Clin. Invest.*, **107**, 1063–1069.
2. Kivirikko, K.I. and Pihlajaniemi, T. (1998) Collagen hydroxylases and the protein disulfide isomerase subunit of prolyl 4-hydroxylases. *Adv. Enzymol Relat. Areas Mol. Biol.*, **72**, 325–398.
3. Myllyharju, J. (2003) Prolyl 4-hydroxylases, the key enzymes of collagen biosynthesis. *Matrix Biol.*, **22**, 15–24.
4. Myllyharju, J. and Kivirikko, K.I. (2004) Collagens, modifying enzymes and their mutations in humans, flies and worms. *Trends Genet.*, **20**, 33–43.
5. Helaakoski, T., Vuori, K., Myllyla, R., Kivirikko, K.I. and Pihlajaniemi, T. (1989) Molecular cloning of the alpha-subunit of human prolyl 4-hydroxylase: the complete cDNA-derived amino acid sequence and evidence for alternative splicing of RNA transcripts. *Proc. Natl. Acad. Sci. USA*, **86**, 4392–4396.
6. Helaakoski, T., Annunen, P., Vuori, K., MacNeil, I.A., Pihlajaniemi, T. and Kivirikko, K.I. (1995) Cloning, baculovirus expression, and characterization of a second mouse prolyl 4-hydroxylase alpha-subunit isoform: formation of an alpha 2 beta 2 tetramer with the protein disulfide-isomerase/beta subunit. *Proc. Natl. Acad. Sci. USA*, **92**, 4427–4431.
7. Annunen, P., Helaakoski, T., Myllyharju, J., Veijola, J., Pihlajaniemi, T. and Kivirikko, K.I. (1997) Cloning of the human prolyl 4-hydroxylase alpha subunit isoform alpha(II) and characterization of the type II enzyme tetramer. The alpha(I) and alpha(II) subunits do not form a mixed alpha(I)alpha(II)beta2 tetramer. *J. Biol. Chem.*, **272**, 17342–17348.
8. Kukkola, L., Hieta, R., Kivirikko, K.I. and Myllyharju, J. (2003) Identification and characterization of a third human, rat, and mouse collagen prolyl 4-hydroxylase isoenzyme. *J. Biol. Chem.*, **278**, 47685–47693.
9. Van Den Diepstraten, C., Papay, K., Bolender, Z., Brown, A. and Pickering, J.G. (2003) Cloning of a novel prolyl 4-hydroxylase subunit expressed in the fibrous cap of human atherosclerotic plaque. *Circulation*, **108**, 508–511.
10. Rauch, F., Fahiminiya, S., Majewski, J., Carrot-Zhang, J., Boudko, S., Glorieux, F., Mort, J.S., Bachinger, H.P. and Moffatt, P. (2015) Cole-Carpenter syndrome is caused by a heterozygous missense mutation in P4HB. *Am. J. Hum. Genet.*, **96**, 425–431.
11. Annunen, P., Autio-Harmainen, H. and Kivirikko, K.I. (1998) The novel type II prolyl 4-hydroxylase is the main enzyme form in chondrocytes and capillary endothelial cells, whereas the type I enzyme predominates in most cells. *J. Biol. Chem.*, **273**, 5989–5992.
12. Nissi, R., Autio-Harmainen, H., Marttila, P., Sormunen, R. and Kivirikko, K.I. (2001) Prolyl 4-hydroxylase isoenzymes I and II have different expression patterns in several human tissues. *J. Histochem. Cytochem.*, **49**, 1143–1153.
13. Helaakoski, T., Veijola, J., Vuori, K., Rehn, M., Chow, L.T., Taillon-Miller, P., Kivirikko, K.I. and Pihlajaniemi, T. (1994) Structure and expression of the human gene for the alpha subunit of prolyl 4-hydroxylase. The two alternatively spliced types of mRNA correspond to two homologous exons the sequences of which are expressed in a variety of tissues. *J. Biol. Chem.*, **269**, 27847–27854.
14. Holster, T., Pakkanen, O., Soininen, R., Sormunen, R., Nokelainen, M., Kivirikko, K.I. and Myllyharju, J. (2007) Loss of assembly of the main basement membrane collagen, type IV, but not fibril-forming collagens and embryonic death in collagen prolyl 4-hydroxylase I null mice. *J. Biol. Chem.*, **282**, 2512–2519.
15. Aro, E., Salo, A.M., Khatri, R., Finnila, M., Miinalainen, I., Sormunen, R., Pakkanen, O., Holster, T., Soininen, R., Prein, C., *et al.* (2015) Severe Extracellular Matrix Abnormalities and Chondrodysplasia in Mice Lacking Collagen Prolyl 4-Hydroxylase Isoenzyme II in Combination with a Reduced Amount of Isoenzyme I. *J. Biol. Chem.*, **290**, 16964–16978.
16. Gonzalez, M.A., Lebrigio, R.F., Van Booven, D., Ulloa, R.H., Powell, E., Speziani, F., Tekin, M., Schule, R. and Zuchner, S. (2013) GEnomes Management Application (GEM.app): a new software tool for large-scale collaborative genome analysis. *Hum. Mutat.*, **34**, 842–846.
17. Lek, M., Karczewski, K., Minikel, E., Samocha, K., Banks, E., Fennell, T., O'Donnell-Luria, A., Ware, J., Hill, A., *et al.* (2015) Analysis of protein-coding genetic variation in 60,706 humans. *Nature*, **536**, 285–291.
18. Pihlajaniemi, T., Myllyla, R. and Kivirikko, K.I. (1991) Prolyl 4-hydroxylase and its role in collagen synthesis. *J. Hepatol.*, **13 Suppl 3**, S2–S7.
19. Jobling, R., D'Souza, R., Baker, N., Lara-Corrales, I., Mendoza-Londono, R., Dupuis, L., Savarirayan, R., Ala-Kokko, L. and Kannu, P. (2014) The collagenopathies: review of clinical phenotypes and molecular correlations. *Curr. Rheumatol. Rep.*, **16**, 394.
20. Cabral, W.A., Chang, W., Barnes, A.M., Weis, M., Scott, M.A., Leikin, S., Makareeva, E., Kuznetsova, N.V., Rosenbaum, K.N., Tifft, C.J., *et al.* (2007) Prolyl 3-hydroxylase 1 deficiency causes a recessive metabolic bone disorder resembling lethal/severe osteogenesis imperfecta. *Nat. Genet.*, **39**, 359–365.
21. Steinmann, B., Royce, P. and Superti-Furga, A. (1993) *The Ehlers-Danlos Syndrome. In Connective tissue and its heritable disorders*. Wiley-Liss, New York, New York.
22. Yis, U., Dirik, E., Chambaz, C., Steinmann, B. and Giunta, C. (2008) Differential diagnosis of muscular hypotonia in infants: the kyphoscoliotic type of Ehlers-Danlos syndrome (EDS VI). *Neuromuscul. Disord.*, **18**, 210–214.
23. Donkervoort, S., Bonnemann, C.G., Loeys, B., Jungbluth, H. and Voermans, N.C. (2015) The neuromuscular differential diagnosis of joint hypermobility. *Am. J. Med. Genet. C. Semin. Med. Genet.*, **169C**, 23–42.
24. Bonnemann, C.G. (2011) The collagen VI-related myopathies: muscle meets its matrix. *Nat. Rev. Neurol.*, **7**, 379–390.

25. Hautala, T., Byers, M.G., Eddy, R.L., Shows, T.B., Kivirikko, K.I. and Myllyla, R. (1992) Cloning of human lysyl hydroxylase: complete cDNA-derived amino acid sequence and assignment of the gene (PLOD) to chromosome 1p36.3—-p36.2. *Genomics*, **13**, 62–69.
26. Dundar, M., Muller, T., Zhang, Q., Pan, J., Steinmann, B., Vodopiutz, J., Gruber, R., Sonoda, T., Krabichler, B., Utermann, G., *et al.* (2009) Loss of dermatan-4-sulfotransferase 1 function results in adducted thumb-clubfoot syndrome. *Am. J. Hum. Genet.*, **85**, 873–882.
27. Ha-Vinh, R., Alanay, Y., Bank, R.A., Campos-Xavier, A.B., Zankl, A., Superti-Furga, A. and Bonafe, L. (2004) Phenotypic and molecular characterization of Bruck syndrome (osteogenesis imperfecta with contractures of the large joints) caused by a recessive mutation in PLOD2. *Am. J. Med. Genet. A*, **131**, 115–120.
28. Salo, A.M., Cox, H., Farndon, P., Moss, C., Grindulis, H., Risteli, M., Robins, S.P. and Myllyla, R. (2008) A connective tissue disorder caused by mutations of the lysyl hydroxylase 3 gene. *Am. J. Hum. Genet.*, **83**, 495–503.
29. Gorres, K.L., Pua, K.H. and Raines, R.T. (2009) Stringency of the 2-His-1-Asp active-site motif in prolyl 4-hydroxylase. *PloS. One*, **4**, e7635.
30. Anantharajan, J., Koski, M.K., Kursula, P., Hieta, R., Bergmann, U., Myllyharju, J. and Wierenga, R.K. (2013) The structural motifs for substrate binding and dimerization of the alpha subunit of collagen prolyl 4-hydroxylase. *Structure*, **21**, 2107–2118.
31. Myllyharju, J. and Kivirikko, K.I. (1997) Characterization of the iron- and 2-oxoglutarate-binding sites of human prolyl 4-hydroxylase. *Embo. J.*, **16**, 1173–1180.
32. Curtin, B.J. and Teng, C.C. (1958) Scleral changes in pathological myopia. *Trans. Am. Acad. Ophthalmol. Otolaryngol.*, **62**, 777–788. discussion 788-790.
33. Curtin, B.J., Iwamoto, T. and Renaldo, D.P. (1979) Normal and staphylomatous sclera of high myopia. An electron microscopic study. *Arch. Ophthalmol.*, **97**, 912–915.
34. Ahmad, N.N., Ala-Kokko, L., Knowlton, R.G., Jimenez, S.A., Weaver, E.J., Maguire, J.I., Tasman, W. and Prockop, D.J. (1991) Stop codon in the procollagen II gene (COL2A1) in a family with the Stickler syndrome (arthro-ophthalmopathy). *Proc. Natl. Acad. Sci. USA*, **88**, 6624–6627.
35. Richards, A.J., Yates, J.R., Williams, R., Payne, S.J., Pope, F.M., Scott, J.D. and Snead, M.P. (1996) A family with Stickler syndrome type 2 has a mutation in the COL11A1 gene resulting in the substitution of glycine 97 by valine in alpha 1 (XI) collagen. *Hum. Mol. Genet.*, **5**, 1339–1343.
36. Vikkula, M., Mariman, E.C., Lui, V.C., Zhidkova, N.I., Tiller, G.E., Goldring, M.B., van Beersum, S.E., de Waal Malefijt, M.C., van den Hoogen, F.H., Ropers, H.H., *et al.* (1995) Autosomal dominant and recessive osteochondrodysplasias associated with the COL11A2 locus. *Cell*, **80**, 431–437.
37. Guo, H., Tong, P., Liu, Y., Xia, L., Wang, T., Tian, Q., Li, Y., Hu, Y., Zheng, Y., Jin, X., *et al.* (2015) Mutations of P4HA2 encoding prolyl 4-hydroxylase 2 are associated with nonsyndromic high myopia. *Genet. Med.*, **17**, 300–306.
38. Teer, J.K., Green, E.D., Mullikin, J.C. and Biesecker, L.G. (2012) VarSifter: visualizing and analyzing exome-scale sequence variation data on a desktop computer. *Bioinformatics*, **28**, 599–600.
39. Kivirikko, K.I. and Myllyla, R. (1982) Posttranslational enzymes in the biosynthesis of collagen: intracellular enzymes. *Methods Enzymol.*, **82 Pt A**, 245–304.
40. Makareeva, E., Mertz, E.L., Kuznetsova, N.V., Sutter, M.B., DeRidder, A.M., Cabral, W.A., Barnes, A.M., McBride, D.J., Marini, J.C. and Leikin, S. (2008) Structural heterogeneity of type I collagen triple helix and its role in osteogenesis imperfecta. *J. Biol. Chem.*, **283**, 4787–4798.